JOURNAL OF APPLIED PHYSICS **106**, 013104 (2009)

Omnidirectional transparency induced by matched impedance in disordered metamaterials

Wei-Hua Sun, Ye Lu, Ru-Wen Peng,[a] Lu-Shuai Cao, De Li, Xin Wu, and Mu Wang
National Laboratory of Solid State Microstructures and Department of Physics, Nanjing University, Nanjing 210093, China

(Received 11 March 2009; accepted 1 June 2009; published online 9 July 2009)

In this work, we present an omnidirectional perfect transmission in the photonic band gap of a metamaterial, where positive-index and active negative-index materials are randomly stacked. Due to mismatched impedance, a photonic band gap appears when the metamaterial possesses zero averaged refractive index. By introducing the matched impedance at the expected frequency, a complete tunneling is achieved in the photonic band gap. This kind of transparency is robust against not only incident angles, optical polarization but system disorder as well. The finding is expected to achieve potential applications in optoelectronic devices. © *2009 American Institute of Physics*. [DOI: 10.1063/1.3159018]

I. INTRODUCTION

In conventional photonic band gap (PBG) materials, Bragg scatterings in a periodically modulated dielectric structure can induce the PBG,[1,2] where the propagation of photons is forbidden. Up until now, PBG materials have achieved wide applications in telecommunication and optoelectronics,[3–6] such as microcavity waveguides and photonic crystal filters. Recently, metamaterials are attracting much interest in constructing PBG materials. A famous example is left-handed materials (LHMs) with negative refractive index, which were suggested theoretically by Veselago in 1968 (Ref. 7) and demonstrated very recently.[8] It is shown that with the assist of LHMs, zero averaged-refractive-index (zero-$\bar{n}$) gap can appear in a stack of positive and negative-index materials.[9] Further, spatial-averaged single-negative (SASN) gap is found in the stack of positive-index and single-negative materials including negative-permittivity or negative-permeability media.[10] Physically, both the zero-$\bar{n}$ gap and the SASN gap originate from the optical path cancellation in those one-dimensional (1D) stacks. Therefore, distinct from the Bragg gap, the zero-$\bar{n}$ gap and the SASN gap are invariant to the geometrical scaling and also insensitive to the incident angle.

Photonic tunneling in the PBG materials is also attractive. Usually the photonic tunneling is related to some resonances.[11,12] For example, due to Fabry–Pérot resonant, some photons can transport through thin metallic slits.[13–15] Extraordinary optical transmission found in the subwavelength hole arrays of metals originates from the resonance between incident light and free electrons, and the excitation of surface plasmon polariton.[16–18] Photonic tunneling can happen in the Bragg gap, when the defects are symmetrically introduced in conventional PBG materials.[19] However, once the light irradiates the sample from normal to oblique incidence, effective optical lengths will change in the media, thereafter, the defect modes shift significantly against incident angles. One may naturally search for the solution to overcome the angular effect. Very recently, Zhou *et al.*[11] demonstrated a type of transparency through negative-permittivity media with high magnetic fields, which is found to have very little dependence on incidence angles. Further by using the resonant coupling of the evanescent-wave-based interface modes, an omnidirectional tunneling mode can be achieved in the photonic heterostructure containing single-negative materials.[20]

In this work, we present another approach based on the impedance-matched effect. We theoretically demonstrate that in a random stack with positive-index (PI) and *active* negative-index (ANI) materials, a wide PBG can be obtained due to the impedance mismatch. By introducing the matched impedance at the frequency of interest, a perfect tunneling appears in the PBG, which is totally independent of incident angles and polarizations of light wave. This paper is organized as follows. In Sec. II, based on Maxwell equations, we present an analytical analysis on omnidirectional perfect transmission in the PBG of the PI/ANI stack, and the requirement for such feature is given. In Sec. III, photonic band structures and optical transmission for periodic and random stacks are numerically calculated. It is demonstrated that the photonic tunneling appears indeed within the band gap, which is robust against incident angles, optical polarization and system disorder in both the dissipation-free system and the dissipation system. Besides, the impact of individual layer thickness on the photonic tunneling in random stacks is discussed. Finally, a summary is given in Sec. IV.

II. THE ANALYTICAL ANALYSIS

A. The perfect transmission mode

We consider the propagation of electromagnetic waves (EMs) in a 1D layered photonic structure, where two materials A and B are randomly arranged along the z axis. Then the stack is characterized by frequency-dependent and space-varying refractive index $n=\sqrt{\varepsilon\mu}$ and impedance $Z=\sqrt{\mu/\varepsilon}$, where $\varepsilon=\varepsilon(z)$ and $\mu=\mu(z)$ are the electric permittivity and

[a]Author to whom correspondence should be addressed. Electronic mail: rwpeng@nju.edu.cn.

the magnetic permeability in the stack. Maxwell equation for the electric field $\boldsymbol{E}$ in the stack can be expressed as

$$\nabla \times \left[\frac{\nabla \times \boldsymbol{E}}{n(z)Z(z)} \right] = \frac{\omega^2}{c^2} \frac{n(z)}{Z(z)} \boldsymbol{E}, \tag{1}$$

where c is the velocity of the EM in vacuum.

Starting from Eq. (1), it is possible to obtain a perfect transmission at the expected frequency in this random stack. For example, if the impedance and the absolute value of the refractive index are constants at certain frequency ω_0, i.e.,

$$\begin{cases} Z(\omega_0, z) = C_1, \\ |n(\omega_0, z)| = C_2, \end{cases} \tag{2}$$

the impedance for the propagation of electromagnetic wave at ω_0 is matched through the stack, and two orthogonal z-component solutions of Eq. (1) can be expressed as $E_0 e^{i(\omega_0/c)\cos\theta \int_0^z n(z')dz'}$ and $E_0' e^{-i(\omega_0/c)\cos\theta \int_0^z n(z')dz'}$, where θ is the incidence angle. Thus by imposing the zero-$\bar{n}$ configuration ($\bar{n} = (1/a)\int_0^a n(z)dz$, where a is the total thickness of the stack and the matched impedance, the electromagnetic wave can transmit through the structure perfectly and result in no phase shift throughout the structure at any incident angle. In this way, an omnidirectional and perfect transmission mode (ω_0) is achieved in the stacking structure due to the matched impedance at this frequency.

B. The requirements for a photonic band gap

The PBG around the perfect transmission mode (ω_0) can be obtained in the disordered binary stack based on Bloch theorem and transfer matrix method.[21] For the transverse electric (TE) or the transverse magnetic (TM) polarization, Maxwell equation in the 1D stack can be rewritten as

$$\frac{d}{dz}\left(\frac{1}{\tilde{P}\tilde{n}} \frac{dU(z)}{dz} \right) + \frac{\tilde{n}\omega^2}{\tilde{P}c^2} U(z) = 0, \tag{3}$$

where $\tilde{n} = \sqrt{\varepsilon\mu \cos^2\theta}$ and $\theta = \theta(z)$ is the angle between the wave vector and the z axis. For TE modes, $U(z)$ stands for the electric field $(E(z))$, and $\tilde{P} \equiv \tilde{Z} = \sqrt{\mu/(\varepsilon \cos^2\theta)}$ is the effective impedance along z; while for TM modes, $U(z)$ stands for the magnetic field $[H(z)]$ and $\tilde{P} \equiv \tilde{G} = \sqrt{\varepsilon/(\mu \cos^2\theta)}$ is the effective conductance along z.

The transfer matrix of both TE and TM waves for the jth layer with thickness d_j can be expressed as

$$T_j(\omega) = \begin{bmatrix} \cos(\tilde{n}_j k d_j) & i\tilde{P}_j \sin(\tilde{n}_j k d_j) \\ i\dfrac{1}{\tilde{P}_j}\sin(\tilde{n}_j k d_j) & \cos(\tilde{n}_j k d_j) \end{bmatrix}. \tag{4}$$

Here $k = \omega/c$ and $\tilde{P}_j$ is the effective impedance/conductance in the jth layer. The transfer matrix for the entire structure (M) can be described by the product of the transfer matrix for each constitutive layer, i.e.,

$$M = \begin{bmatrix} 1 & 1 \\ -1/\tilde{P}_i & 1/\tilde{P}_i \end{bmatrix}^{-1} \times (\Pi_{j=1}^N T_j) \times \begin{bmatrix} 1 & 1 \\ -1/\tilde{P}_t & 1/\tilde{P}_t \end{bmatrix} \equiv \begin{bmatrix} m_1 & m_2 \\ m_3 & m_4 \end{bmatrix}, \tag{5}$$

where $\tilde{P}_i$ and $\tilde{P}_t$ are the effective impedance/conductance for the incident medium and transmitted medium, respectively. Therefore, the reflection and transmission of the structure can be expressed as

$$R = \left| \frac{m_3}{m_1} \right|^2,$$

$$T = \frac{\tilde{P}_i}{\tilde{P}_t} \left| \frac{1}{m_1} \right|^2, \tag{6}$$

respectively.

Due to the fact that there is no translational invariance in random systems, the Bloch theorem cannot be directly applied. However, by taking the particular disordered stack as "one primitive cell" in a periodic system,[22] we can apply the Bloch theorem as $E(z+a) = e^{iqa}E(z)$ to deduce the condition for a PBG in the stack. (Here a is the total thickness of the disordered stack.) Thereafter, in the case of

$$\mathrm{Tr}[T(\omega)] = 2\cos(qa) > 2, \tag{7}$$

the propagation of electromagnetic waves at the frequency of ω is forbidden in the structure.

C. Photonic band gap in a periodic stacking

If we consider the subwavelength limit, i.e., the wavelength is much larger than the optical length of constitutive layer, a forbidden gap in the binary periodic stacking can be obtained only if

$$\mathrm{Tr}(T(\omega)) \cong 2 - k^2 \times \left[(\tilde{n}_A d_A)^2 + (\tilde{n}_B d_B)^2 + \left(\frac{\tilde{P}_A}{\tilde{P}_B} + \frac{\tilde{P}_B}{\tilde{P}_A} \right) \tilde{n}_A \tilde{n}_B d_A d_B \right] > 2 \tag{8}$$

is satisfied.[10] Here d_A and d_B are the thickness of layer A and B, respectively.

Now we go to the stack, where layer A is a conventional PI material while layer B is a NI material. We assume that material A is dispersionless (n_A=const) and material B is dispersive $[n_B(\omega)]$, and $d_A = d_B = d$ for simplicity. At the perfect transmission mode (ω_0), $n_A = -n_B(\omega_0)$, $\varepsilon_A = -\varepsilon_B(\omega_0)$, $\mu_A = -\mu_B(\omega_0)$, and $|\theta_A| = |\theta_B| = \theta$. Around the frequency ω_0, we have $\mathrm{Tr}[T(\omega)] \cong 2 - k^2 d^2 \cos^2\theta[\varepsilon_A + \varepsilon_B(\omega)][\mu_A + \mu_B(\omega)]$. Thereafter, the requirement for the photonic band gap around ω_0 is given by

$$\frac{\partial \varepsilon_B}{\partial \omega} \times \frac{\partial \mu_B}{\partial \omega} < 0. \tag{9}$$

Therefore, once layer B has an opposite dispersion characteristics of the electric permittivity and the magnetic permeability around the frequency ω_0, there exists the impedance mismatch of A and B in the stack, then a PBG is achieved around ω_0.

D. Photonic band gap in a random stacking

In a random binary stacking, we can directly follow Ref. 9 to prove that a PBG (zero-$\bar{n}$) can also be achieved. In this case, the electric field inside the structure can be decomposed as forward and backward components. We assume that the effective impedance is mismatched in the structure and it has a variation around the perfect transmission mode (ω_0). Based on Bloch theorem, the mismatched impedance in the zero-$\bar{n}$ stack leads to imaginary q.[9] Therefore, a PBG can be obtained around the perfect transmission mode (ω_0) once Eq. (9) is satisfied in a disordered stack.

Physically, for both periodic and random zero-$\bar{n}$ stackings, the matched impedance corresponds to a tunneling mode at ω_0 according to Eq. (2), while the mismatched impedance to a PBG around ω_0 according to Eq. (9).

III. NUMERICAL CALCULATIONS AND DISCUSSIONS

Based on Eqs. (4)–(7), we have carried out the numerical calculations on photonic band structure and optical transmission of the PI/ANI stacks. In our calculation, the PI material (layer A) is assumed to be nondispersive, the permittivity and the permeability are set as $\varepsilon_A=4$ and $\mu_A=1$, respectively. The ANI material (layer B) is dispersive, its permittivity and permeability follows the Lorentz model as[23]

$$\varepsilon_B(\omega) = 1 - \frac{K}{\omega^2 - \omega_{e0}^2 + i\gamma_e\omega},$$

$$\mu_B(\omega) = 1 - \frac{F}{\omega^2 - \omega_{p0}^2 + i\gamma_p\omega}, \tag{10}$$

where ω_{e0} is the electronic resonance frequency and ω_{p0} is the magnetic resonance frequency; K and F are constants. It is known that in conventional passive media, both K and F are positive, and γ corresponds to dissipation; thus both $\partial\varepsilon_B/\partial\omega$ and $\partial\mu_B/\partial\omega$ are positive in the normal-dispersion region or negative in the abnormal dispersion region. Equation (9) can be satisfied in passive media when the normal-dispersion zone of ε overlaps with the abnormal dispersion zone of μ or vice versa. Meanwhile, as we will demonstrate below, in *active* materials with abnormal dispersion such as an inverted two-level system,[24–26] K is smaller than zero and γ corresponds to optical gain, thus $\partial\varepsilon_B/\partial\omega<0$. Then at some frequencies, Eq. (9) is satisfied in the stack, i.e., opposite dispersion characteristics of the permittivity and the permeability around the frequency ω_0 are achieved in the ANI material (layer B) (as shown in Fig. 1). We will show a perfect transmission appearing within a wide impedance-mismatched PBG in a random PI/ANI stack.

Figures 2(a) and 2(b) present the photonic band structures for the periodic PI/ANI stack and the random stack, respectively. It is shown that in both cases, a transmission mode appears at ω_0 within a wide band gap, which is invariant against the incident angle and optical polarization (the

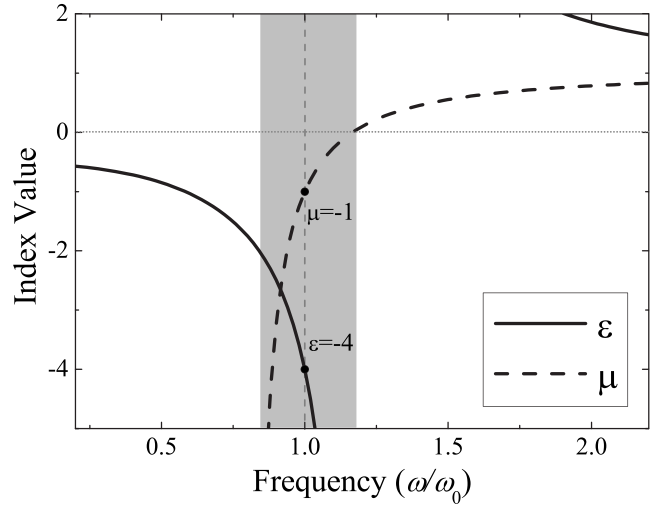

FIG. 1. The electric permittivity (ε) and the magnetic permeability (μ) of the ANI material, which is for layer B in the stack. Standard Lorentz model [Eq. (10)] was taken to describe the dispersion, where $K=2.2\pi^2\times10^{30}$ $(\text{rad/s})^2$ and $\omega_{e0}=12\pi\times10^{14}$ rad/s for the permittivity, while $F=7.2\pi^2\times10^{29}$ $(\text{rad/s})^2$ and $\omega_{p0}=8\pi\times10^{14}$ rad/s for the permeability, the damping factors are ignored in this case. The shaded area highlights the negative-index frequency region. Please note that at $\omega_0=\pi\times10^{15}$ rad/s, $\varepsilon_B=-4$, and $\mu_B=-1$, where the matched impedance will be achieved through the PI/ANI stack.

TE mode or the TM mode). At the frequency ω_0, we have $\varepsilon_A=-\varepsilon_B$ and $\mu_A=-\mu_B$ in the PI/ANI stack. Then, the impedance is matched when the photon with the frequency of ω_0 propagates in the stack. As a consequence, the photonic tun-

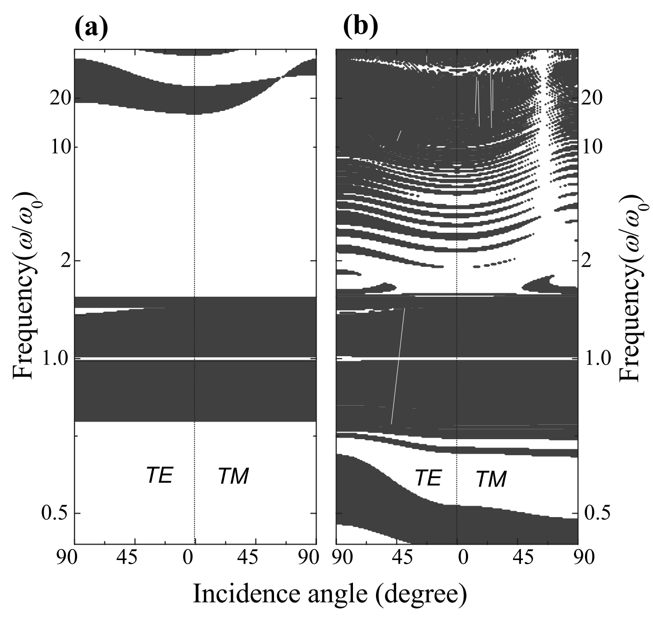

FIG. 2. The calculated photonic band structures of the periodic (a) and the random (b) PI/ANI stacks in terms of frequency ω and incident angle θ. There are two types of layers: layer A and layer B. Layer A is a dispersion-free and PI material, its index is assumed to be $\varepsilon_A=4$ and $\mu_A=1$; while layer B is an ANI material and it possesses the dispersion property illustrated in Fig. 1. The thickness for each layer is set as $d=d_A=d_B=5$ nm and there are 80 layers totally in the stacking. Note that, in each figure, the left part is for the TE mode, while the right part for the TM mode. Moreover the white area stands for allowed photonic bands, while the dark area for forbidden gaps. An omnidirectional tunneling mode is shown at ω_0 in both periodic and random stacks.

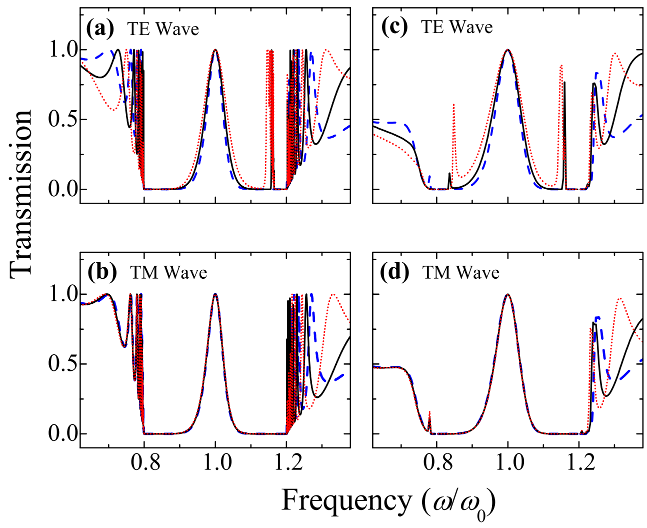

FIG. 3. (Color online) The transmission spectra of the periodic [(a) and (b)] and the random [(c) and (d)] PI/ANI stacks for both the TE mode and the TM mode at different incidences. The material and structural parameters are the same as those in Fig. 2. In each figure, the blue dashed line is for normal incidence ($\theta=0°$), the black solid line for $\theta=45°$ and the red dotted line for $\theta=89°$. In both stacks, there always is a transmission peak at the frequency of ω_0 for different incidence angles and different polarizations.

neling is achieved in the stack when the photonic frequency is at ω_0. Interestingly, this photonic tunneling lies in a wide zero-$\bar{n}$ band gap, which originates from the mismatched impedance. Actually at this region, the permittivity and the permeability of layer B satisfy Eq. (9) indeed. Meanwhile in the higher frequency region, the band structure is dominated by Bragg scattering, which is different from zero-$\bar{n}$ band gap and very sensitive to system disorder and incident angles (as shown in Fig. 2).

The transmission spectra in the TE mode and the TM mode are also investigated for the periodic and random PI/ANI stacks at different incidences [as shown in Figs. 3(a)–3(d)]. In both stacks, there always is a transmission peak at the frequency of ω_0 for different incident angles and different polarizations [Figs. 3(a)–3(d)]. However, the transmission far away from ω_0 is governed by Bragg scattering and presents large variation with the change of incidence angle. In order to show clearly photonic tunneling in the PI/ANI stack, the electric field distributions in the stack are calculated for different frequencies (as shown in Fig. 4). It is obvious that the electromagnetic wave with the frequency of ω_0 can propagate through the whole stack without any decay in both periodic [Fig. 4(a)] and random [Fig. 4(c)] cases. Once the frequencies are deviated from ω_0, the electromagnetic wave may exponentially decay in the stack for the periodic [Fig. 4(b)] and also the random [Fig. 4(d)] cases.

The omnidirectional transmission at ω_0 is also robust against the scale change in the PI/ANI stack. For example, if the thickness of each layer in the stack varies within the subwavelength frame, the omnidirectional perfect transmission can always be found at the same frequency (ω_0). However, increasing the layer thickness may lead to a significant change in the quality factor Q of the transmission peak, which is defined as $Q=\lambda_0/\Delta\lambda$. Here λ_0 is the wavelength of the peak and $\Delta\lambda$ is the half width of the peak. It is found that

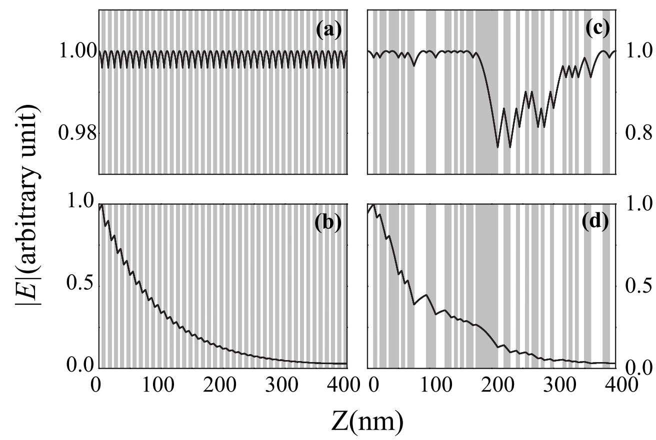

FIG. 4. The field distributions along the z axis in the period PI/ANI stacking at the frequency: (a) $\omega=\omega_0$ and (b) $\omega=1.1\omega_0$. While the field distributions in the random PI/ANI stacking at the frequency: (c) $\omega=\omega_0$ and (d) $\omega=1.1\omega_0$. The material and structural parameters are the same as those in Fig. 2.

the quality factor of the transmission peak at ω_0 will increase if the layer thickness increases [as shown in Fig. 5(a)], which originates from stronger multiple scatterings in the stack. The enhancement in quality factor of the peak is also observed in oblique incidence for both TE and TM polarizations [Figs. 5(b) and 5(c)]. This feature opens up a new possibility for constructing a new type of filters for electromagnetic waves.

It is also worthwhile for us to consider the dissipation system, where material B possesses dissipation and gain

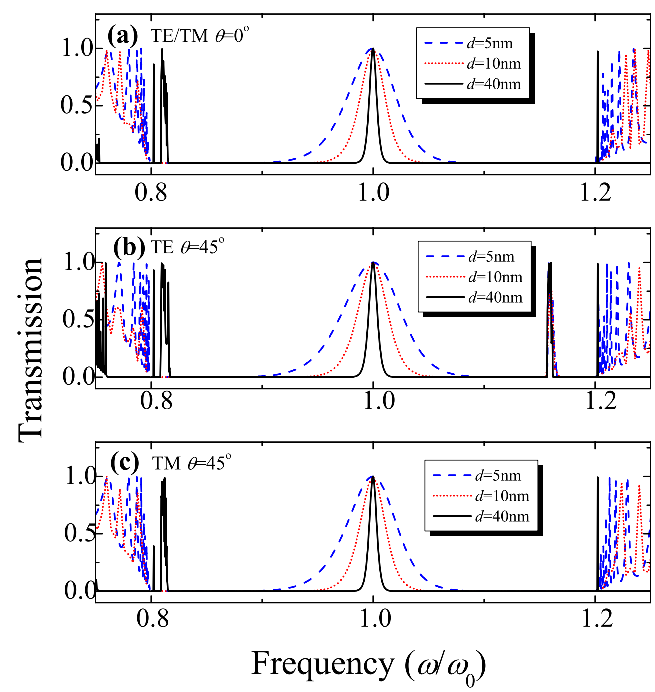

FIG. 5. (Color online) The transmission spectra of the periodic PI/ANI stacks with scale change for different incidence angle θ. (a) $\theta=0$, (b) TE mode at $\theta=45°$, and (c) TM mode at $\theta=45°$. In each figure, the blue dashed line is for the stack with the individual layer thickness $d=5$ nm, the red dotted line for $d=10$ nm, and the black solid line for $d=40$ nm, respectively. The other parameters are the same as those in Fig. 2. The omnidirectional perfect transmission can be found at the same frequency (ω_0), and the quality factor of the transmission peak increases as the layer thickness increases.

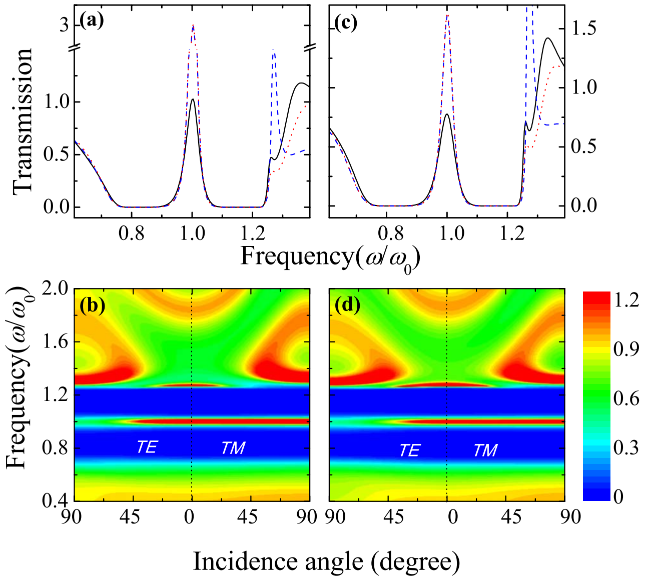

FIG. 6. (Color online) The transmission spectra and the maps of transmission of the periodic and random PI/ANI stacks when the loss and the gain of material B are considered. The damping factor of ε_B and μ_B for material B are chosen to be $\gamma_e=4\pi\times10^{13}$ rad/s and $\gamma_p=8\pi\times10^{13}$ rad/s. The other parameters are the same as those in Fig. 2. In the transmission spectra of (a) the periodic and (c) the random stacks, the blue dashed line is for normal incident, the black solid line for TE mode at $\theta=45°$, and the red dotted line for TM mode at $\theta=45°$, respectively. While the maps of transmission are for (b) the periodic and (d) the random stacks, respectively.

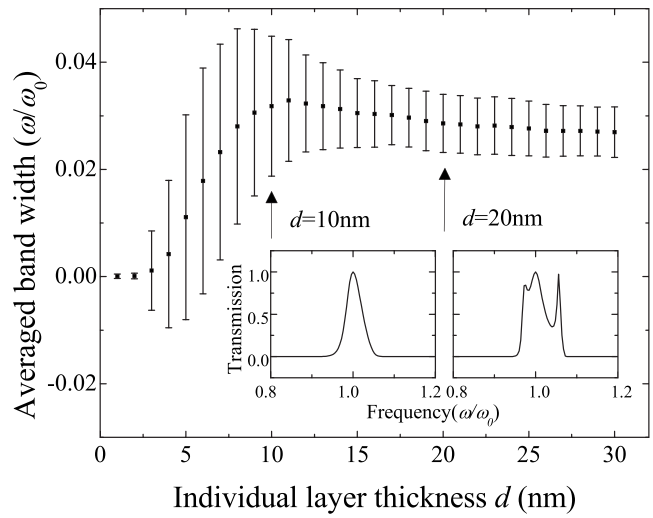

FIG. 7. The averaged band width of the 400-layer random PI/ANI stacks for normal incident as a function of individual layer thickness d. The other parameters are the same as those in Fig. 2. The averaging was taken over 1000 realizations. Two typical transmission spectra ($d=10$ nm and $d=20$ nm) are shown in the inset.

since it is unavoidable in realization.[27,28] In the following calculation, the damping factors for ε_B and μ_B in Eq. (10) are chosen to be $\gamma_e=0.4$ and $\gamma_p=0.5$, respectively. It is shown that the omnidirectional transmission still appears at the frequency of ω_0 within a zero-$\bar{n}$ gap in the periodic and random stacks [as shown in Figs. 6(a) and 6(c)]. Although the frequency for photonic tunneling is the same as that in Fig. 3, the intensity of the transmission peak changes with incident angle because the dispersion property of material B has incorporated dissipation and gain. Besides, the TM wave transmits more powerfully than the TE wave does. It should be noted that at certain frequencies, the intensity of the transmission peak is larger than one. This feature indicates that the optical gain, which is inherent to our structure, wins over the dissipation at those frequencies in the whole structure.[27,29] Furthermore, the maps of transmission are illustrated in Fig. 6(b) for the periodic stack and in Fig. 6(d) for the random stack, respectively. It can be seen that the transmission intensities are stronger for the periodic stack than those in the random one. Anyway, it is obvious that the omnidirectional transparency within the photonic band gap can also be found in the PI/ANI stacks where the dissipation is involved.

Besides, it is true that the subwavelength approximation is taken in the analytical analysis in Sec. II. In practice, the numerical calculations show that for the periodic stack, the tunneling transmission exists even when individual layer thickness (d) reaches approximately 1/5 of the incident wavelength before the transmission mode joins another band; while for random stacking cases, the transmission peak breaks into a band when d exceeds about 1% of the incident wavelength. And beyond that limit, the transmission spectrum becomes configuration dependent and is inclined to distortion. We show in Fig. 7 the averaged band width for the random stackings with different d. The averaging was taken over 1000 realizations. With the increase of d, the tunneling mode grows into a pass band. Two typical transmission spectra are plotted in the inset of Fig. 7. It can be seen that for smaller d (for example, $d=10$ nm) the perfect transmission is intact; however, as d becomes larger (for example, $d=20$ nm) the transmission peak expands and becomes distorted. Such phenomena can be attributed to a lack of phase accumulation over the structure which is due to the phase cancellation across alternating PI and ANI layers as reported in Ref. 30.

Finally, it should be mentioned that the omnidirectional transparency within the photonic band gap can also be achieved in the stacks with the single-negative-index material. For example, if layer A becomes a negative ε-dispersive *active* material and layer B becomes a negative μ-dispersive medium, the photonic band structures and the optical transmission are the same as those in the above PI/ANI stacks.

IV. CONCLUSION

In conclusion, we have presented an approach in achieving omnidirectional transmission through the stacking of conventional positive refractive index material and *active* negative refractive index material. It is found that due to mismatched impedance, a PBG appears when the stack possesses zero averaged refractive index, while by introducing the matched impedance at the expected frequency; a complete tunneling is achieved in the photonic band gap. This kind of transparency is robust against incidence angles and system disorder. The numerical calculations are in good agreement with the analytical predictions. We expect that the findings may achieve potential applications in optoelectronic devices.

ACKNOWLEDGMENTS

This work was supported by grants from the National Natural Science Foundation of China (Grant Nos. 10625417, 50672035, and 10874068), the State Key Program for Basic Research from the Ministry of Science and Technology of China (Grant Nos. 2004CB619005 and 2006CB921804), and partially by the Ministry of Education of China and Jiangsu Province (Grant Nos. NCET-05-0440 and BK2008012). Two of the authors (W.-H.S. and Y.L.) contributed equally to this work.

[1]S. John, Phys. Rev. Lett. **58**, 2486 (1987).
[2]E. Yablonovitch, Phys. Rev. Lett. **58**, 2059 (1987).
[3]J. S. Foresi, P. R. Villeneuve, J. Ferrera, E. R. Thoen, G. Steinmeyer, S. Fan, J. D. Joannopoulos, L. C. Kimerling, H. I. Smith, and E. P. Ippen, Nature (London) **390**, 143 (1997).
[4]J. D. Joannopoulos, P. R. Villeneuve, and S. Fan, Nature (London) **386**, 143 (1997).
[5]A. Mekis, J. C. Chen, I. Kurland, S. Fan, P. R. Villeneuve, and J. D. Joannopoulos, Phys. Rev. Lett. **77**, 3787 (1996).
[6]J. Zi, J. Wan, and C. Zhang, Appl. Phys. Lett. **73**, 2084 (1998).
[7]V. G. Veselago, Sov. Phys. Usp. **10**, 509 (1968).
[8]J. B. Pendry, A. J. Holden, D. J. Robbins, and W. J. Stewart, IEEE Trans. Microwave Theory Tech. **47**, 2075 (1999); J. B. Pendry, Phys. Rev. Lett. **85**, 3966 (2000); R. A. Shelby, D. R. Smith, and S. Schultz, Science **292**, 77 (2001); J. Valentine, S. Zhang, T. Zentgraf, E. Ulin-Avila, D. A. Genov, G. Bartal, and X. Zhang, Nature (London) **455**, 376 (2008).
[9]J. Li, L. Zhou, C. T. Chan, and P. Sheng, Phys. Rev. Lett. **90**, 083901 (2003).
[10]Y. I. Weng, Z.-G. Wang, and H. Chen, Phys. Rev. E **75**, 046601 (2007).
[11]L. Zhou, W. J. Wen, C. T. Chan, and P. Sheng, Phys. Rev. Lett. **94**, 243905 (2005).
[12]Y. Fang and S. He, Phys. Rev. A **78**, 023813 (2008).
[13]F. Yang and J. R. Sambles, Phys. Rev. Lett. **89**, 063901 (2002).
[14]Y. Takakura, Phys. Rev. Lett. **86**, 5601 (2001).
[15]J. A. Porto, F. J. García-Vidal, and J. B. Pendry, Phys. Rev. Lett. **83**, 2845 (1999).
[16]T. W. Ebbesen, H. J. Lezec, H. F. Ghaemi, T. Thio, and P. A. Wolff, Nature (London) **391**, 667 (1998); W. L. Barnes, A. Dereux, and T. W. Ebbesen, *ibid.* **424**, 824 (2003); C. Genet and T. W. Ebbesen, *ibid.* **445**, 39 (2007).
[17]Z. H. Tang, R. W. Peng, Z. Wang, X. Wu, Y. J. Bao, Q. J. Wang, Z. J. Zhang, W. H. Sun, and M. Wang, Phys. Rev. B **76**, 195405 (2007); Y. J. Bao, R. W. Peng, D. J. Shu, M. Wang, X. Li, J. Shao, W. Lu, and N. B. Ming, Phys. Rev. Lett. **101**, 087401 (2008).
[18]A. Battula, S. Chen, Y. Lu, R. J. Knize, and K. Reinhardt, Opt. Lett. **32**, 2692 (2007).
[19]R. W. Peng, X. Q. Huang, F. Qiu, M. Wang, A. Hu, S. S. Jiang, and M. Mazzer, Appl. Phys. Lett. **80**, 3063 (2002).
[20]G. Guan, H. Jiang, H. Li, Y. Zhang, H. Chen, and S. Zhu, Appl. Phys. Lett. **88**, 211112 (2006).
[21]M. Kohmoto, B. Sutherland, and K. Iguchi, Phys. Rev. Lett. **58**, 2436 (1987).
[22]A. P. Vinogradov and A. M. Merzlikin, Phys. Rev. E **70**, 026610 (2004).
[23]N. W. Ashcroft and N. D. Mermin, *Solid State Physics* (Brooks Cole, Belmont, 1976).
[24]R. W. Boyd, *Nonlinear Optics* (Academic, New York, 2003).
[25]R. Y. Chiao, Phys. Rev. A **48**, R34 (1993).
[26]Y. F. Chen, P. Fischer, and F. W. Wise, Phys. Rev. Lett. **95**, 067402 (2005).
[27]Y. F. Chen, P. Fischer, and F. W. Wise, J. Opt. Soc. Am. B **23**, 45 (2006).
[28]R. Y. Chiao and J. Boyce, Phys. Rev. Lett. **73**, 3383 (1994).
[29]L. J. Wang, A. Kuzmich, and A. Dogariu, Nature (London) **406**, 277 (2000).
[30]A. A. Asatryan, L. C. Botten, M. A. Byrne, V. D. Freilikher, S. A. Gredeskul, I. V. Shadrivov, R. C. McPhedran, and Y. S. Kivshar, Phys. Rev. Lett. **99**, 193902 (2007).